Superhydrophobic Effect

DOI: 10.1002/ange.200602126

Photoinduced Reversible Formation of Microfibrils on a Photochromic Diarylethene Microcrystalline Surface**

Kingo Uchida, Norikazu Izumi, Shinichiro Sukata, Yuko Kojima, Shinichiro Nakamura,* and Masahiro Irie*

Lotus and taro leaves have hydrophobic surfaces, which in nature consist of micrometer-scale rods or projections that exhibit a super water-repellent property called the lotus effect. The contact angle of a water droplet on such surfaces is 161.0 ± 2.7°. Recently, many reports concerning changes in water droplet contact angle as a result of changes in surface morphology and surface polarity have been published.[1] Additionally, changes in photoresponsive wettability have also been reported.[2]

Herein, we report a new photoinduced change in surface morphology that provides superhydrophobic properties, obtained by the photoinduced reversible formation of fine fibril structures on coated microcrystalline surfaces. The origin of the reversible formation of fibrils is the photoisomerization of a photochromic diarylethene molecule **1** (see Scheme 1) of a thin film. The reversible changes in surface morphology of a thin film made from photochromic diarylethene **1** were followed by scanning electron microscopy (SEM), optical microscopy, and contact angle measurements of a water droplet. The film was prepared by coating a solution of **1** in chloroform onto a substrate, which gave a contact angle of the water droplet of around 120°. Upon irradiation with UV light, the film surface became superhydrophobic (contact angle 163°). SEM images showed that the surface was covered with microfibrils of diameter around 1 µm. Upon irradiation with visible light, the surface again became flat and recovered the initial contact angle of 120°.

Diarylethene derivatives are promising artificial photoresponsive molecules that show reversible transformation between open- and closed-ring isomers with different absorption spectra.[3] As they also show thermally irreversible and fatigue-resistant photochromic performance,[4] intensive studies have aimed at applications such as molecular memories and switches.[5–13] Herein, we report a new function for the cast film of a derivative.

There are two approaches to controlling surface wettability. One is to change the surface morphology, because it is known that increasing surface roughness results in a superhydrophobic surface, an effect that is widely observed on lotus leaves.[14,15] Such micrometer-scale rugged or fractal structures were also artificially prepared to make superhydrophobic surfaces.[1b,16,17] The other approach is a change of polarity.[18–22] Several reports have attempted to control surface wettability by using photochromic compounds that change the surface polarity.[21] We report changes in photoinduced wettability based on the changes in morphology of a photochromic diarylethene crystal and thin film.

The photochromism of a diarylethene, 1,2-bis(2-methoxy-5-trimethylsilylthien-3-yl)perfluorocyclopentene (**1o**; Scheme 1), in a hexane solution is shown in the Supporting Information. The open-ring isomer is colorless, and absorption maxima of the spectrum were observed at $\lambda = 255$ ($\varepsilon = 2.8 \times 10^4\,\text{M}^{-1}\text{cm}^{-1}$) and 325 nm ($\varepsilon = 7.7 \times 10^3\,\text{M}^{-1}\text{cm}^{-1}$). Upon UV irradiation (254 nm), the solution turned blue and a new band was observed at 599 nm ($\varepsilon = 5.2 \times 10^3\,\text{M}^{-1}\text{cm}^{-1}$). Upon irradiation with visible light, the color disappeared and the bands of the open-ring isomer were regenerated (see Scheme 1). The coloration and discoloration quantum yields were 0.37 and 0.0015, respectively. The reversible formation of the two isomers was not only observed in solution but also in the crystalline phase.

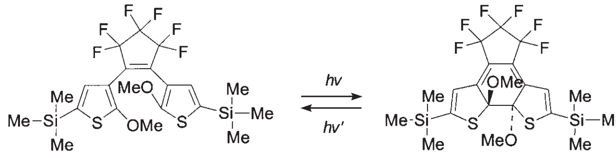

Open-ring isomer **1o** Closed-ring isomer **1c**

Scheme 1. Reversible formation of open-ring isomer **1o** and closed-ring isomer **1c**.

An SEM image of the crystalline surface is shown in Figure 1a. Upon UV irradiation (254 nm), the color became deep blue within 5 min, yet no change in surface morphology was observed at this moment at room temperature. After irradiation for 10 min the crystal was stored in the dark, but 5 min later small microfibrils had already started to grow (see

---

[*] Prof. K. Uchida, N. Izumi, S. Sukata
Department of Materials Chemistry
Faculty of Science and Technology, Ryukoku University and
CREST, Japan Science and Technology Corporation
Seta, Otsu 520-2194 (Japan)
Fax: (+81) 77-543-7483
E-mail: uchida@chem.ryukoku.ac.jp
Homepage: http://www.chem.ryukoku.ac.jp/~uchida/UchidaLab5a.htm

Dr. Y. Kojima, Dr. S. Nakamura
Mitsubishi Chemical Group
Science and Technology Research Center, Inc. and
CREST, Japan Science and Technology Corporation
1000 Kamoshida, Yokohama 227–8502 (Japan)
E-mail: shin@cc.m-kagaku.co.jp

Prof. M. Irie
Department of Chemistry and Biochemistry
Graduate School of Engineering, Kyushu University
6-10-1 Hakozaki, Fukuoka 812-8581 (Japan)

[**] This work was partly supported by Grants-in-Aid for Scientific Research (B) (18350101) from the Ministry of Education, Culture, Sports, Science, and Technology (MEXT) of the Japanese Government. We thank Prof. Takahiro Seki and Mitsuo Hara for the powder X-ray analysis. We also express thanks to Prof. Hiroshi Komatsu, Prof. Tsuyoshi Tsujioka, Dr. Takao Matsuzaki, Prof. Nobuo Niimura, Dr. Seiya Kobatake, and S. Matsumoto for their helpful discussions.

Supporting information for this article is available on the WWW under http://www.angewandte.org or from the author.

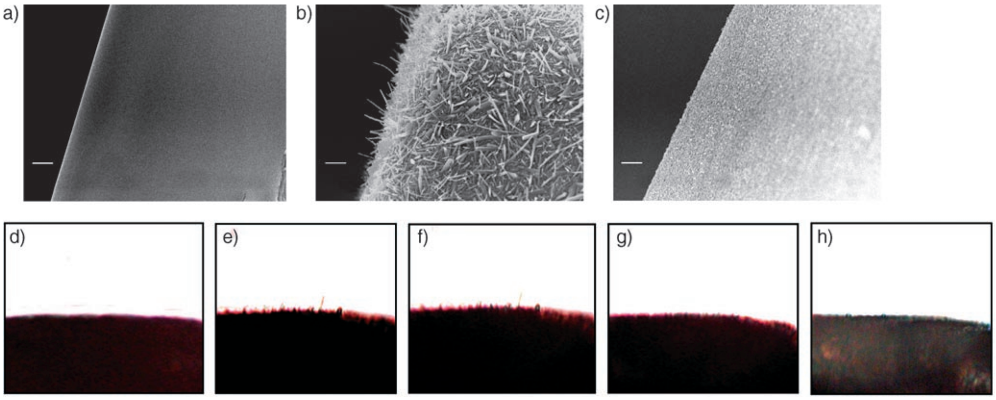

Figure 1. Reversible changes in surface morphology of a single crystal of **1** (scale bar: 10 μm). a) SEM image of the crystal surface of **1o** from a side view (×1000) before UV irradiation (254 nm). b) SEM image from a side view (×1000) of the surface after UV irradiation (254 nm, 12 W, 10 min) and storage in the dark for 24 h. c) SEM image from a side view (×1000) of the surface after irradiation with visible light ($\lambda > 500$ nm, 500 W, 20 min) and storage in the dark for 24 h. d–h) Optical microscopic images (×500) of the appearance and disappearance of fibrils upon irradiation with UV and visible light (500-W Xe lamp, $\lambda > 500$ nm). d) Before irradiation with UV light, the surface was flat. e) After UV irradiation (254 nm, 10 min) and storage in the dark for 5 h at room temperature, microfibrils were generated. Irradiation with visible light for f) 5, g) 10, and h) 60 min.

Supporting Information). After storage for 24 h, the surface was covered with many microfibrils, as shown in Figure 1 b. Upon irradiation of the surface with visible light ($\lambda > 500$ nm), the blue color and the microfibrils disappeared (see Figure 1 c). The surface changes at the same point were also monitored from a side view by using an optical microscope (see Figure 1 d–h). The disappearance process (Figure 1 e–h) of the fibrils was well monitored.

Measurement of the contact angle of a water droplet is a simple and direct method for evaluating wettability. The contact angle of the film surface before UV irradiation was 120° (Figure 2 a). Upon irradiation of the surface with UV light (254 nm), the color became blue and the angle was reduced to around 90° (Figure 2 b) after a short irradiation time (1–2 min). After 24 h the angle had gradually increased to 163° (Figure 2 c and d).

The colored surface was irradiated with visible light to regenerate the open-ring isomer. After 20 min the blue color disappeared. The contact angle was also monitored during the fibril disappearing process. It gradually decreased and finally recovered to the initial 120° (Figure 2 e).

Powder X-ray diffraction measurements were carried out to elucidate the composition of the microfibrils. Figure 3 shows a comparison of the measured powder diffraction patterns and estimated patterns from single-crystal structure analysis of the open- (**1o**) and closed-ring (**1c**) isomers. The fibril pattern was in good agreement with that of the closed-ring isomer. Diffraction peaks at 5.1, 7.7, and 15.0° are appropriate for the (001), (010), and $(1\bar{1}\bar{1})$ lattice planes of the closed-ring isomer crystal, respectively. Ordinarily, closed-ring isomers formed in the crystal of open-ring isomers are strained by the lattice and have different structures from closed-ring isomer crystals obtained by recrystallization in solution.[23,24] The above results indicate that the fibril crystal formed on the film grew freely from the crystal lattice of the open-ring isomer.

The phase diagram of photoirradiated crystals was measured to investigate why microfibrils grew after UV irradiation (Figure 4). The melting points of the open- and closed-ring isomers are 99.8–100.3 and 143.2–144.1 °C, respectively, whereas the melting point of the mixture of open- and closed-ring isomers decreased to around 30 °C at a certain ratio (24:76 open-ring/closed-ring isomers). The result suggests that a homocrystal of the closed-ring isomer is formed from the melting of the crystal at this ratio.

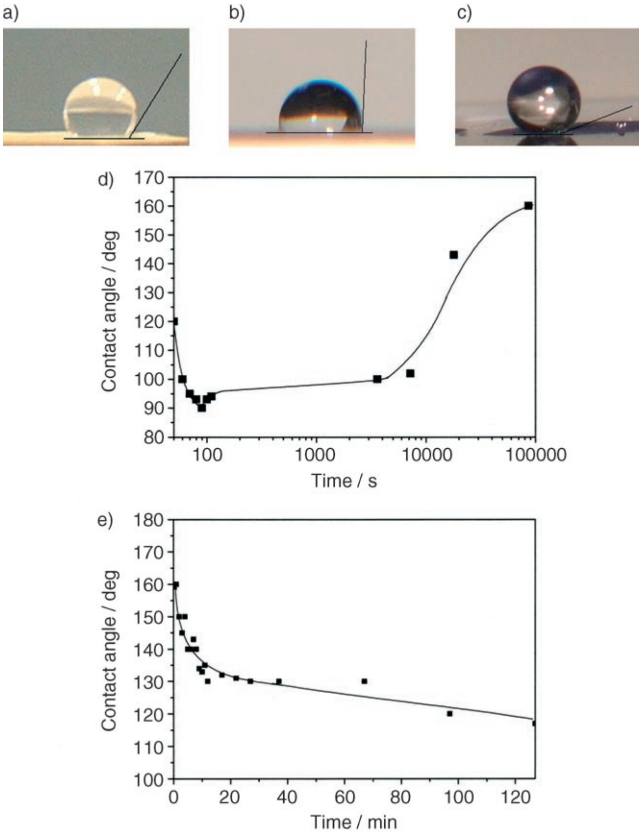

Figure 2. Contact angles of a water droplet on a microcrystalline film of diarylethene **1**. a) Water droplet (1.2 mm ∅) on the microcrystalline surface before irradiation with UV light (254 nm, 12 W). The contact angle was 120 ± 2°. b) Water droplet after UV irradiation for a short time (1–2 min). The contact angle changed to 92 ± 2°. c) Water droplet after irradiation (10 min) with light and storage in the dark at room temperature for 24 h. The contact angle increased to 163 ± 2°. d) Time profile of the contact angle during the fibril generation process after UV irradiation. e) Profile during fibril disappearance upon irradiation of the colored fibril structured surface with visible light.

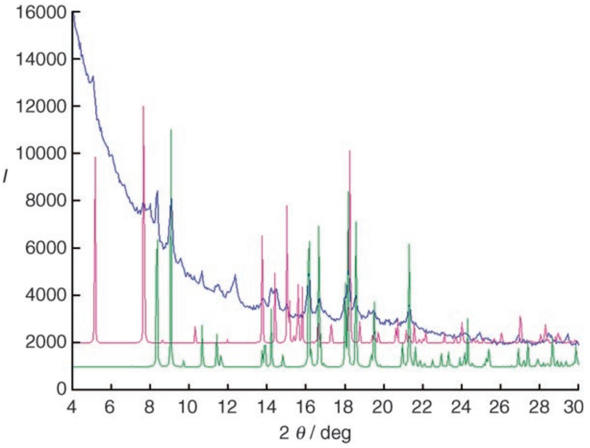

Figure 3. X-ray diffraction patterns of needles obtained from the surface by scratching (blue line), and of **1o** (green line) and **1c** (pink line) derived from single-crystal analysis.

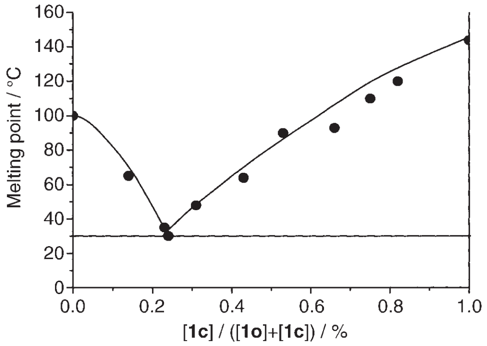

Figure 4. Phase diagram of mixtures of open- (**1o**) and closed-ring isomers (**1c**) formed by irradiation of diarylethene crystals with UV light (313 nm).

The shape of the crystals of the closed-ring isomer was a needle or fibril when obtained by recrystallization from a solution containing this isomer. The crystal shape tends to grow in one direction along the *a* axis. Upon UV irradiation, the open-ring isomer is converted to the closed-ring isomer. When conversion exceeds 24 %, crystal growth of the closed-ring isomer starts to form fibril structures on the film surface. To confirm this mechanism, the sample was kept in air and water at different temperatures. Below around 0 °C the fibril did not grow, but we found fibril formation in water and in air around 30 °C. The results also support the melt mechanism as depicted in the phase diagram. Fibril growth was not only observed on glass and metal substrates but also on plastics and paper. The film will be applicable to materials with photoinduced reversible surface water repellency.

Experimental Section

The preparation of **1o** and **1c** is described in detail in the Supporting Information. Single crystals of **1o** and **1c** were obtained by recrystallization from ethanol. A solution of **1o** in chloroform (100 mg mL^{-1}) was coated on the substrate (glass, resin, or metal), and the solvent was evaporated. The film thickness was approximately 20–30 μm and was measured by observing the scratched surface by SEM.

A scanning electron microscope (JEOL JSM-5200) and an optical microscope (Leica DMLP) were used to study the surface microstructure. Photoirradiation (visible light: $\lambda > 500$ nm) was carried out using a Ushio 500-W xenon lamp with a cutoff filter (Toshiba color filter Y-50), and UV irradiation was carried out by using a Topcon UV lamp PU-2 (12 W). X-ray crystallographic analysis was performed using a Bruker SMART CCD X-ray diffractometer. Suitable colorless prism-shaped (**1o**) and dark blue needle crystals (**1c**) were obtained by recrystallization from ethanol. Crystals with dimensions of $0.5 \times 0.4 \times 0.15$ mm^3 (**1o**) and $0.5 \times 0.1 \times 0.05$ mm^3 (**1c**) were mounted on a glass fiber and aligned on a Bruker SMART 1000 CCD diffractometer (platform with full three-circle goniometer) at room temperature. The diffractometer was equipped with a 1K CCD detector set 50.0 mm from each crystal. Intensity measurements were performed using graphite-monochromated Mo$_{K\alpha}$ radiation from a sealed ceramic diffraction tube (Siemens). Generator settings were 50 kV/40 mA. SMART was used for preliminary determination of the unit cell constants and data collection control. The intensities of the reflections of the hemisphere were collected by a combination of three sets of exposures (frames). Each set had a different angle ϕ for the crystal and each exposure covered a range of 0.3° in ω; 1800 frames were collected for each crystal with an exposure time of 5.0 s per frame for **1o** and 10.0 s per frame for **1c**. Data integration and global cell refinement was performed with SAINT. The final unit cells were obtained after integration from the *xyz* centroids of 2912 reflections for **1o** and 1352 reflections for **1c**. Intensity data were corrected for Lorentz and polarization effects, scale variation, and decay and absorption; based on the intensities of symmetry-related reflections measured at different angular settings (SADABS), multiscan absorption correction was applied and reduced to F_o^2.

Crystal data and structural refinement parameters for **1o**: $C_{21}H_{26}F_6O_2S_2Si_2$, $M_r = 544.72$, triclinic, space group $P\bar{1}$, $a = 10.122(6)$, $b = 11.268(6)$, $c = 12.814(7)$ Å, $\alpha = 103.355(11)$, $\beta = 94.298(13)$, $\gamma = 74.981(12)°$, $V = 1373.3(13)$ Å^3, $Z = 2$, $\rho_{calcd} = 1.317$ g cm^{-3}, $\mu(Mo_{K\alpha}) = 0.337$ mm^{-1}, $T = 298(2)$ K, $F(000) = 564$, $R1 = 0.0685$ ($wR2 = 0.2056$) for 5717 unique reflections ($R_{int} = 0.0172$) with a GOF of 0.927. Crystal data and structural refinement parameters for **1c**: $C_{21}H_{26}F_6O_2S_2Si_2$, $M_r = 544.72$, triclinic, space group $P\bar{1}$, $a = 6.697(2)$, $b = 11.777(4)$, $c = 17.470(6)$ Å, $\alpha = 96.899(6)$, $\beta = 96.993(6)$, $\gamma = 98.472(6)°$, $V = 1339.2(8)$ Å^3, $Z = 2$, $\rho_{calcd} = 1.351$ g cm^{-3}, $\mu(Mo_{K\alpha}) = 0.346$ mm^{-1}, $T = 298(2)$ K, $F(000) = 564$, $R1 = 0.0791$, ($wR2 = 0.1898$) for 4496 unique reflections ($R_{int} = 0.0359$) with a GOF of 0.883. Data were collected on a Bruker SMART 1000 CCD diffractometer with graphite-monochromated Mo$_{K\alpha}$ radiation ($\lambda = 0.71073$ Å). The structure was solved by direct methods using SHELXS97 and refined by full-matrix least-squares against F^2 with SHELXL97.[25] CCDC 293161 (**1o**) and 293162 (**1c**) contain the supplementary crystallographic data for this paper. These data can be obtained free of charge from the Cambridge Crystallographic Data Centre via www.ccdc.cam.ac.uk/data_request/cif.

Received: May 28, 2006

Keywords: crystal growth · hydrophobic effect · photochromism · thin films

---

[1] a) H. Y. Erbil, A. L. Demirel, Y. Avci, O. Mert, *Science* **2003**, *299*, 1377 – 1380; b) T. Onda, S. Shibuichi, N. Satoh, K. Tsujii, *Langmuir* **1996**, *12*, 2125 – 2127.

[2] a) S. Wang, X. Feng, J. Yao, L. Jiang, *Angew. Chem.* **2006**, *118*, 1286 – 1289; *Angew. Chem. Int. Ed.* **2006**, *45*, 1264 – 1267; b) H. Liu, L. Feng, J. Zhai, L. Jiang, D. Zhu, *Langmuir* **2004**, *20*, 5659 – 5661.

[3] a) G. H. Brown, *Photochromism*, Wiley-Interscience, New York, **1971**; b) H. Duerr, H. Bouas-Laurent, *Photochromism: Molecules and Systems*, Elsevier, Amsterdam, **1990**.
[4] a) M. Irie, *Chem. Rev.* **2000**, *100*, 1685 – 1716; b) M. Irie, K. Uchida, *Bull. Chem. Soc. Jpn.* **1998**, *71*, 985 – 996.
[5] M. Irie, K. Uchida, T. Eriguchi, H. Tsuzuki, *Chem. Lett.* **1995**, 899 – 900.
[6] S. Kobatake, T. Yamada, K. Uchida, N. Kato, M. Irie, *J. Am. Chem. Soc.* **1999**, *121*, 2380 – 2386.
[7] S. Kobatake, M. Yamada, T. Yamada, M. Irie, *J. Am. Chem. Soc.* **1999**, *121*, 8450 – 8456.
[8] T. Yamada, S. Kobatake, K. Muto, M. Irie, *J. Am. Chem. Soc.* **2000**, *122*, 1589 – 1592.
[9] M. Irie, T. Lifka, S. Kobatake, N. Kato, *J. Am. Chem. Soc.* **2000**, *122*, 4871 – 4876.
[10] S. Kobatake, K. Shibata, K. Uchida, M. Irie, *J. Am. Chem. Soc.* **2000**, *122*, 12135 – 12141.
[11] S. Kobatake, K. Uchida, E. Tsuchida, M. Irie, *Chem. Commun.* **2002**, 2804 – 2805.
[12] M. Morimoto, S. Kobatake, M. Irie, *Chem. Rec.* **2004**, *4*, 23 – 38.
[13] M. Irie, S. Kobatake, M. Horichi, *Science* **2001**, *291*, 1769 – 1772.
[14] W. Barthlott, C. Neinhuis, *Planta* **1997**, 202, 1 – 8.
[15] C. Neinhuis, W. Barthlott, *New Phytol.* **1998**, *138*, 91 – 98.
[16] H. Y. Erbil, A. L. Demirel, Y. Avci, O. Mert, *Science* **2003**, *299*, 1377 – 1380.
[17] S. Shibuichi, T. Onda, N. Satoh, K. Tsujii, *J. Phys. Chem.* **1996**, *100*, 19512 – 19517.
[18] X. Feng, J. Zhai, L. Jiang, *Angew. Chem.* **2005**, *117*, 5245 – 5248; *Angew. Chem. Int. Ed.* **2005**, *44*, 5115 – 5118.
[19] S. Abbott, J. Ralston, G. Reynolds, R. Hayes, *Langmuir* **1999**, *15*, 8923 – 8928.
[20] J. Lahann, S. Mitragotri , T.-N. Tran, H. Kaido, J. Sundaram, I. S. Choi, S. Hoffer, G. A. Somorjai, R. Langer, *Science* **2003**, *299*, 371 – 374.
[21] K. Ichimura, S.-K. Oh, M. Nakagawa, *Science* **2000**, *288*, 1624 – 1626.
[22] B. S. Gallardo, V. K. Gupta, F. D. Eagerton, L. I. Jong, V. S. Craig, R. R. Shah, N. L. Abbott, *Science* **1999**, *283*, 57 – 60.
[23] T. Yamada, S. Kobatake, M. Irie, *Bull. Chem. Soc. Jpn.* **2000**, *73*, 2179 – 2184.
[24] S. Kobatake, M. Morimoto, Y. Asano, A. Murakami, S. Nakamura, M. Irie, *Chem. Lett.* **2002**, *31*, 1224 – 1225.
[25] SHELXS97 and SHELXL97, G. M. Sheldrick, Programs for Crystal Structure Analysis, University of Göttingen, Germany, **1997**.